Stress Intensity Factors for Viscoelastic Axisymmetric Problems Applied to Wood

Rostand Moutou Pitti, Claude Chazal, Florence Labesse-Jied, Yuri Lapusta

STRESS INTENSITY FACTORS FOR VISCOELASTIC AXISYMMETRIC PROBLEMS APPLIED TO WOOD

Rostand MOUTOU PITTI[1,2,5], Claude CHAZAL[3], Florence LABESSE-JIED[1,2], Yuri LAPUSTA[2,4]

[1]Clermont Université, Université Blaise Pascal, Institut Pascal, BP 10448,
F-63000 Clermont-Ferrand, France
[2]CNRS, UMR 6602, Institut Pascal, F-63171 Aubière, France
[3]GEMH Laboratory, Université de Limoges, Centre Universitaire Génie Civil
19300 Egletons, France
[4]Clermont Université, IFMA, Institut Pascal, BP 10448, F-63000 Clermont-Ferrand, France
[5]CENAREST, IRT, BP 14070, Libreville, Gabon

rostand.moutou.pitti@polytech.univ-bpclermont.fr

ABSTRACT. Many materials used in engineering applications obey to time-dependent behaviours and the mechanical fields are affected by the time effects. As a result, the evolution of the stresses and strains in these materials appear still very complex and difficult to study. Among such cases is the situation when the material has an axisymmetric shape and when it is submitted to a complex fracture loading. In this paper, the creep loading is applied on an axisymmetric viscoelastic orthotropic material and the stress intensity factors are computed in the opening mode, in the shear mode and in the mixed mode using to a finite element approach. The uncoupling method is based on M integral, combining the virtual and real mechanical fields. In the same time, the viscoelastic effects are introduced according to the generalized Kelvin-Voigt model composed by four branches. The numerical solution is obtained with an incremental viscoelastic formulation in the time domain. Using a Compact Tension Shear (CTS) specimen, the evolutions of stress intensity factor versus time are posted in each fracture mode configuration. The obtained results demonstrate the efficiency of the proposed model.

1. Introduction

Modern advanced materials like composites, bi-materials, polymers and also soft materials are strongly present in the mechanical and civil engineering industries and play an important role in the integrity and resistance of structures. An important factor in their serviceability is the crack initiation and growth (see e.g. [1-3]. In industrial applications, one of the important cases is the symmetry of revolution. It is often present in nuclear power plants [4], engines or flying equipments [5,6]. Also, the symmetry of revolution is typical in the wood used in individual or industrial houses [7]. In this case, the material is submitted to fracture under mixed-mode loading combined with viscoelastic behaviour [8,9], which remains a complex problem.

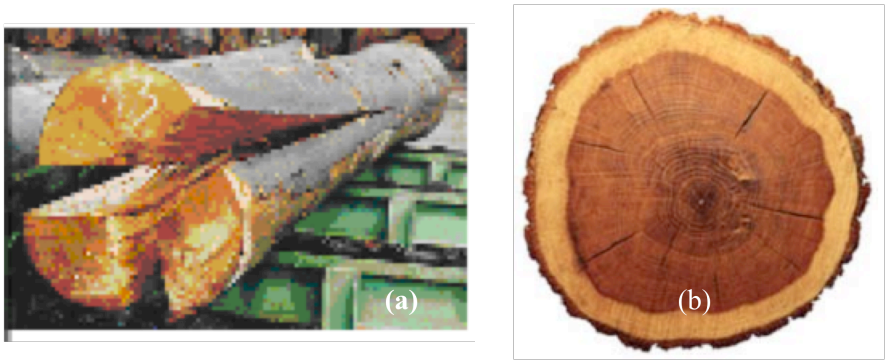

Figure 1 – (a) Crack in cylindrical peace of wood. (b) Cross section of wood

In the literature, some developments have been suggested to approach such problems. Among them, numerical solutions have been proposed to resolve the time-dependent material behaviour with Maxwell equations [10]. Also, according to non-

dependent integrals, a generalization of the M integral [11] and T and A integrals to viscoelastic materials have been proposed in order to resolve the axisymmetric problem submitted to environmental loading [12]. The main advantage of this last approach is to compute the real mechanical fields in a virtual configuration and uncoupling fracture and viscoelastic parameters. In this paper an adaptation of these integrals to the case of viscoelastic problems in axisymmetric configurations like wood materials is developed.

According to figure 1 (a), the fracture process is an important fact of the collapse of peace of wood using in the timber building. It observed that after the cut, the wood is often exposed in open air and submitted to environmental and climate loading during a long time [13]. With the drying cycle actions, the micro cracks are initiated and can propagate under the creep loading when the wood is used as timber structures. Also, the cracks are often oriented from the center to the boundary of the sample, see figure 1 (a). The observed cracks can be explained by the orthotropic character, the cellular composition of the specie, but also by its viscoelastic behaviour combined with the axisymmetric property. This paper is strongly motivated by the necessity to study such an interesting behaviour.

Firstly, the conservative laws and the Langrangian variation is recalled in order to introduce the bilinear form of free energy density [14,15] and the virtual extension crack in cylindrical coordinates [16]. Also, the independent path integrals *M* [11] is defined and generalized to axisymmetric configuration. Secondly, the integral is defined to viscoelastic behaviour according to the generalized Kelvin Voigt chain. In order to introduce the numerical fracture process in mixed-mode configuration, the Compact Tension Shear specimen is applied. The last part proposes the viscoelastic incremental law routine and the evolutions of stress intensity factors and viscoelastic energy release rate versus the each mixed mode ratio.

2. Background of axisymmetric integral parameters

2.1 Lagrangian conservation

According to Moutou Pitti et al. [16], for cracked domain *V*, the Noether's theorem [15] translates that the Langrangian variation is equal to zero for all time *t* chosen arbitrary and for all real δu and virtual δv displacement fields:

$$\delta L = \int_t \int_V \delta F^{\bullet} \, \mathrm{d}t \, \mathrm{d}V = 0 \qquad \text{with} \quad F(u,v) = F^{\bullet} \tag{1}$$

In the case of Arbitrary Euleurian Langrangian configuration, we have the following notations [11]

$$\delta\tilde{v}_i = \delta v_i \; ; \;\; \delta\tilde{v}_i = 0 \; ; \;\; \delta\tilde{v}_i = \delta v_i + \delta v_i^* \;\; ; \;\; \delta\tilde{u}_i = \delta u_i \; ; \;\; \delta\tilde{u}_i = 0 \; ; \;\; \delta\tilde{u}_i = \delta u_i + \delta u_i^* \tag{2}$$

where $\tilde{v}$ and v^* are virtual Euleurian and Lagrangian (ALE) displacement fields, respectively. Using relation (2), and considering the virtual extension vector $\vec{\kappa}\delta a$, where *a* is a crack length, the Langrangian (1) becomes:

$$\delta L = \int_t \int_V \left(\frac{\partial F^{\bullet}}{\partial u_{i,j}} \delta u_{i,j} + \frac{\partial F^{\bullet}}{\partial u_{i,j}} \delta u^*_{i,j} + \frac{\partial F^{\bullet}}{\partial v_{i,t}} \delta v_{i,t} + \frac{\partial F^{\bullet}}{\partial v_{i,t}} \delta v^*_{i,t} \right) \kappa_k \, \delta a \, \mathrm{d}t \;\; \mathrm{d}V \tag{3}$$

According to equations (2), the virtual displacement gradient can be written as:

$$\delta u_{i,j} = \frac{\partial u_{i,j}}{\partial x_k} \kappa_k \delta a \; ; \quad \delta v_{i,j} = \frac{\partial v_{i,j}}{\partial x_k} \kappa_k \delta a \; ; \quad \delta u_{i,t} = \frac{\partial u_{i,t}}{\partial x_k} \kappa_k \delta a \; ; \quad \delta v_{i,t} = \frac{\partial v_{i,t}}{\partial x_k} \kappa_k \delta a \tag{4}$$

Using equations (4), the bilinear free energy density (1) becomes

$$\begin{aligned}
&\frac{\partial F^{\bullet}}{\partial u_{i,j}} \cdot \delta u^*_{i,j} = \left(\frac{\partial F^{\bullet}}{\partial u_{i,j}} \cdot \delta u^*_i \right)_{,j} - \left(\frac{\partial F^{\bullet}}{\partial u_{i,j}} \right)_{,j} \cdot \delta u^*_i ; \quad \frac{\partial F^{\bullet}}{\partial u_{i,t}} \cdot \delta u^*_{i,t} = \left(\frac{\partial F^{\bullet}}{\partial u_{i,t}} \cdot \delta u^*_i \right)_{,t} - \left(\frac{\partial F^{\bullet}}{\partial u_{i,t}} \right)_{,t} \cdot \delta u^*_i \\
&\frac{\partial F^{\bullet}}{\partial v_{i,j}} \cdot \delta v^*_{i,j} = \left(\frac{\partial F^{\bullet}}{\partial v_{i,j}} \cdot \delta v^*_i \right)_{,j} - \left(\frac{\partial F^{\bullet}}{\partial v_{i,j}} \right)_{,j} \cdot \delta v^*_i ; \quad \frac{\partial F^{\bullet}}{\partial v_{i,t}} \cdot \delta v^*_{i,t} = \left(\frac{\partial F^{\bullet}}{\partial v_{i,t}} \cdot \delta v^*_i \right)_{,t} - \left(\frac{\partial F^{\bullet}}{\partial v_{i,t}} \right)_{,t} \cdot \delta v^*_i
\end{aligned} \tag{5}$$

By introducing expressions (5) in the Lagrangian (3), and applying the Gauss - Ostrogradski theorem leads to

$$\begin{aligned}\delta L = &\int_t \int_V \frac{\partial F^{\bullet}}{\partial x_k} \kappa_k \, \delta a \, \mathrm{d}t \; \mathrm{d}V + \int_t \int_{\partial V} \left(\frac{\partial F^{\bullet}}{\partial u_{i,j}} u_{i,k} + \frac{\partial F^{\bullet}}{\partial v_{i,j}} v_{i,k} \right) \kappa_k \, n_j \, \delta a \; \mathrm{d}t \; \mathrm{d}S \\ &- \int_V \left(\frac{\partial F^{\bullet}}{\partial u_{i,t}} u_{i,k} + \frac{\partial F^{\bullet}}{\partial v_{i,t}} v_{i,k} \right) \kappa_k \, \delta a \; \mathrm{d}V + \int_t \int_V \left(\left(\frac{\partial F^{\bullet}}{\partial u_{i,j}} \right)_{,j} u_{i,k} + \left(\frac{\partial F^{\bullet}}{\partial v_{i,j}} \right)_{,j} v_{i,k} \right) \kappa_k \, \delta a \; \mathrm{d}t \; \mathrm{d}V \\ &+ \int_t \int_V \left(\left(\frac{\partial F^{\bullet}}{\partial u_{i,j}} \right)_{,j} u_{i,k} + \left(\frac{\partial F^{\bullet}}{\partial v_{i,j}} \right)_{,j} v_{i,k} \right) \kappa_{k,j} \, \delta a \; \mathrm{d}t \; \mathrm{d}V + \int_t \int_V \left(\left(\frac{\partial F^{\bullet}}{\partial u_{i,t}} \right)_{,t} u_{i,k} + \left(\frac{\partial F^{\bullet}}{\partial v_{i,t}} \right)_{,t} v_{i,k} \right) \kappa_k \, \delta a \; \mathrm{d}t \; \mathrm{d}V \end{aligned} \tag{6}$$

∂V designates the boundary curve of V or a closed contour around the crack tip, composed by the specific contours [11,16].

2.2 Axisymmetric integral

According to the equation (6) and the non-dependent domain and without pressure on the crack lips as proposed by [16], we can write after mathematical transformation:

$$\begin{aligned} M_{axi} = &\frac{1}{2} \int_{\Gamma_1} \left(\sigma^{v}_{ij,k} \cdot u_i - \sigma^{u}_{ij} \cdot v_{i,k} \right) \kappa_k \, n_j \; \mathrm{d}\Gamma_1 \\ &+ \frac{1}{2} \int_V \left(\left(\sigma^{v}_{ij} \left(u_{i,j} \right)_{,k} + \sigma^{u}_{ij} \left(v_{i,j} \right)_{,k} \right) - \left(\left(\sigma^{v}_{ij} u_{i,j} \right)_{,k} + \left(\sigma^{u}_{ij} v_{i,j} \right)_{,k} \right) \right) \kappa_{k,j} \, \mathrm{d}V \end{aligned} \tag{7}$$

The integral (7) is defined with a curvilinear integration domain. In order to implement this integral in a finite element software, it is easier to take into account a surface domain integral. In this context, the curvilinear domain must be transformed by introducing a vector field $\vec{\theta}$ [11,12]. After simplification, we obtain the modelling form of M_{axi} integral called $M\theta_{axi}$ adapted to axisymmetric problem.

$$\begin{aligned} M\theta_{axi} = &\frac{1}{2} \int_{\Omega} \left(\sigma^{u}_{ij} \cdot v_{i,k} - \sigma^{v}_{ij,k} \cdot u_i \right) \theta_{k,j} \; \kappa_k \, \mathrm{d}V \\ &+ \frac{1}{2} \int_{\Omega} \left(\left(\sigma^{v}_{ij} \left(u_{i,j} \right)_{,k} + \sigma^{u}_{ij} \left(v_{i,j} \right)_{,k} \right) - \left(\left(\sigma^{v}_{ij} \cdot u_{i,j} \right)_{,k} + \left(\sigma^{u}_{ij} \cdot v_{i,j} \right)_{,k} \right) \right) \theta_k \, \kappa_{k,j} \, \mathrm{d}V \end{aligned} \tag{8}$$

The first term of (8) provides the mixed mode separation for a stationary crack and integrates the axisymmetric aspect. The second term traduces the dissipated energy induced by the crack-growth process.

3. Generalization to viscoelastic behaviour

In the case of creep loading, the linear viscoelastic behaviour is based on a generalized Kelvin Voigt model composed by N cells of Kelvin Voigt associated with a spring in series, see Figure 2.

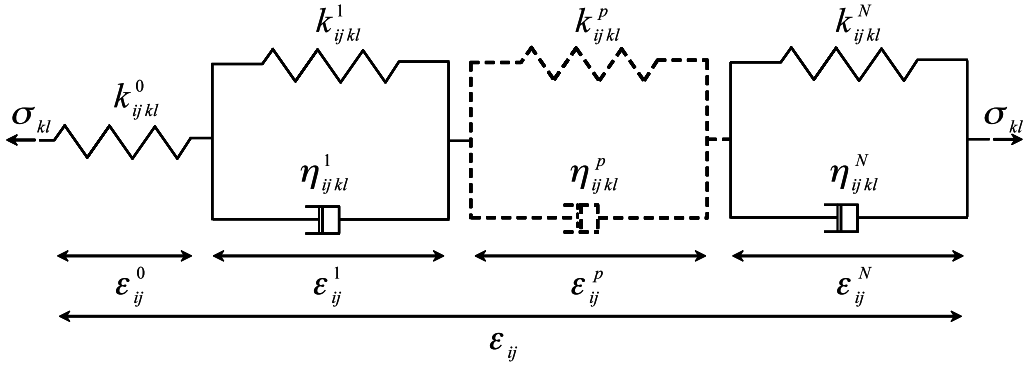

Figure 2 – Generalized Kelvin Voigt model

In this case, the Equation (9) can be generalized for each elastic property as follows:

$$M\theta v_{axi} = \frac{1}{2}\int_{\Omega}\left({}^{(p)}\sigma_{ij}^{u}\cdot v_{ij}^{(p)} - {}^{(p)}\sigma_{ij,k}^{v}\cdot u_{i}^{(p)}\right)\theta_{k,j}\,\kappa_{k}\,\mathrm{d}V + \frac{1}{2}\int_{\Omega}\left(\left({}^{(p)}\sigma_{ij}^{v}\left(u_{i,j}^{(p)}\right)_{,k} + {}^{(p)}\sigma_{ij}^{u}\left(v_{i,j}^{(p)}\right)_{,k}\right) - \left(\left({}^{(p)}\sigma_{ij}^{v}\cdot u_{i,j}^{(p)}\right)_{,k} + \left({}^{(p)}\sigma_{ij}^{u}\cdot v_{i,j}^{(p)}\right)_{,k}\right)\right)\theta_{k}\,\kappa_{k,j}\,\mathrm{d}V \tag{9}$$

${}^{(p)}\sigma_{ij}^{u}$ and ${}^{(p)}\sigma_{ij}^{v}$ indicate the real and virtual stresses of the p^{th} spring respectively, induced by mechanical and thermal fields. $u_i^{(p)}$ and $v_i^{(p)}$ are real and virtual displacement fields in the p^{th} spring respectively. For an orthotropic media, virtual field $v^{(p)}$ is given by the Sih's singular form. According to equation (9), the real stress intensity factors are given by:

$${}^{u}K_{I}^{(p)} = 8\cdot\frac{M\theta v_{axi}^{(p)}\left({}^{v}K_{I}^{(p)}=1\,,\,{}^{v}K_{II}^{(p)}=0\right)}{C_{1}^{(p)}} \quad \text{and} \quad {}^{u}K_{II}^{(p)} = 8\cdot\frac{M\theta v_{axi}^{(p)}\left({}^{v}K_{I}^{(p)}=0\,,\,{}^{v}K_{II}^{(p)}=1\right)}{C_{2}^{(p)}} \tag{10}$$

Finally, the viscoelastic energy release rate in each fracture mode are given by

$$G_{v}^{(p)} = {}^{1}G_{v}^{(p)} + {}^{2}G_{v}^{(p)} = C_{1}^{(p)}\cdot\frac{\left({}^{u}K_{I}^{(p)}\right)}{8} + C_{2}^{(p)}\cdot\frac{\left({}^{u}K_{II}^{(p)}\right)}{8} \tag{11}$$

${}^{1}G_{v}^{(p)}$ and ${}^{2}G_{v}^{(p)}$ are the energy release rate of the p^{th} spring in mode I and II respectively. $C_1^{(p)}$ and $C_2^{(p)}$ designate the associate viscoelastic compliance.

4. Numerical results

4.1 Axisymmetric plan and Compact Tension Shear specimen

In the axisymmetric configuration, the circular crack evolution and the integration domain are posted in Figure 3 [17]. The crack tip is oriented in the radial direction and the continuum map θ surrounds the cracked surface.

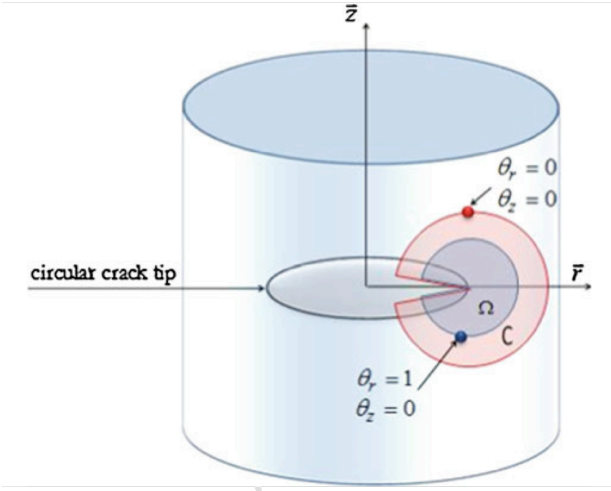

Figure 3 – Crack growth position in axysimmetric plan [17]

In order to compute the stress intensity factors in the axisymmetric material, a modified CTS specimen, Figure 4, proposed by Moutou Pitti et al. [16] for orthotropic material has been considered. This specimen is used in computational finite elements to generate the different mixed-mode ratios. The initial square form specimen is replaced by the cylindrical form with the diameter $d = 100\ mm$ and the initial crack length $a = 50\ mm$. The loading points A_α and B_α with $\alpha \in (1\ldots 7)$ are oriented according to the angle solicitation β. The pure mode I $(\beta = 0°)$ is obtained by using opposite forces in A_1 and B_1, the pure mode II by the loading points A_7 and B_7 (β = 90°).

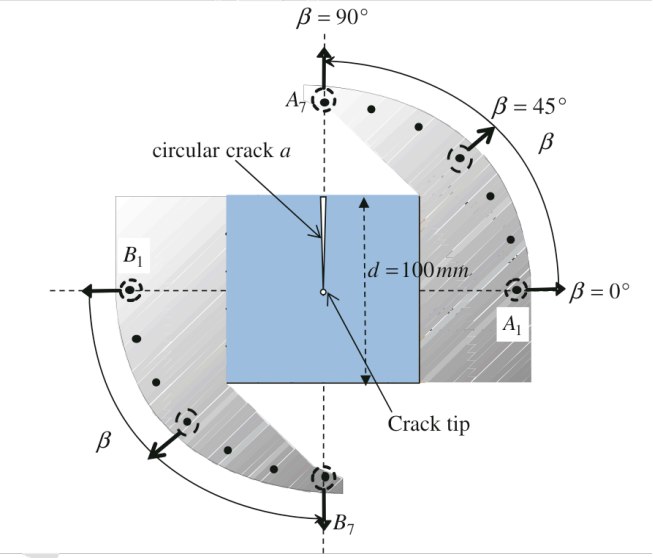

Figure 4 – Compact Tension Shear specimen [16].

4.2 Numerical routine

Figure 5 presents the viscoelastic incremental and the fracture routine implemented in finite element software Castem.

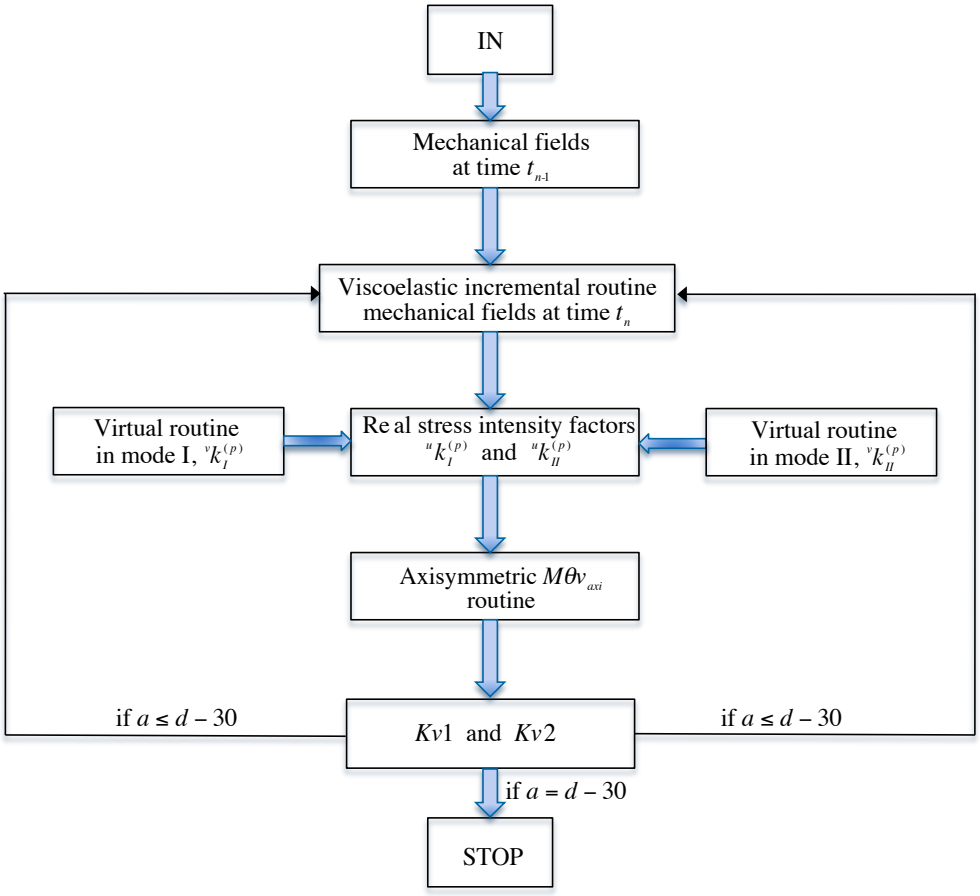

Figure 5 – Viscoelastic incremental and fracture routine

- In the beginning, the elastic mechanical fields are computed at time t_{n-1} with the initial circular crack length $a = 50mm$, posted in Figure 4. Also, the representative circular mesh in the axisymmetric configuration is shown in Figure 3.
- At the following crack length $a = 51\ mm$, the viscoelastic incremental formulation proposed by [11] [16] [18] is applied in order to compute the viscoelastic mechanical fields at time t_n. In the fact, the Boltzmann equation introduced with the generalized Kelvin Voigt model (Figure 2) is resolved step by step in finite element process.
- Simultaneously, the compliance factors, the virtual stress intensity factors in opening ${}^{v}K_I^{(p)}$ and in shear mode [15] have calculated according to the crack virtual procedure. Then, the real stress intensity factor ${}^{u}K_I^{(p)}$ and ${}^{u}K_I^{(p)}$ obtained by considering the equation (10).
- The real stress intensity factors are introduced in the axisymmetric $M\theta v_{axi}$ routine according to the relation (9). Then, using the equation (11), the viscoelastic stress intensity factors in opening mode *kv1* and in shear mode *kv2* for the axisymmetric materials are evaluated. The precedent steps are repeated until the final collapse of the wood material with the crack length $a = 70$.

4.3 Stress intensity factor and energy release rate

In the numerical finite element calculation, the stress plan configuration is considered. The creep function, the elastic orthotropic moduli of the pine spruce are considered with a constant Poisson coefficient $\upsilon = 0.3$, see Moutou Pitti et al. [16] and three Kelvin Voigt cells have been used according to the Figure 2.

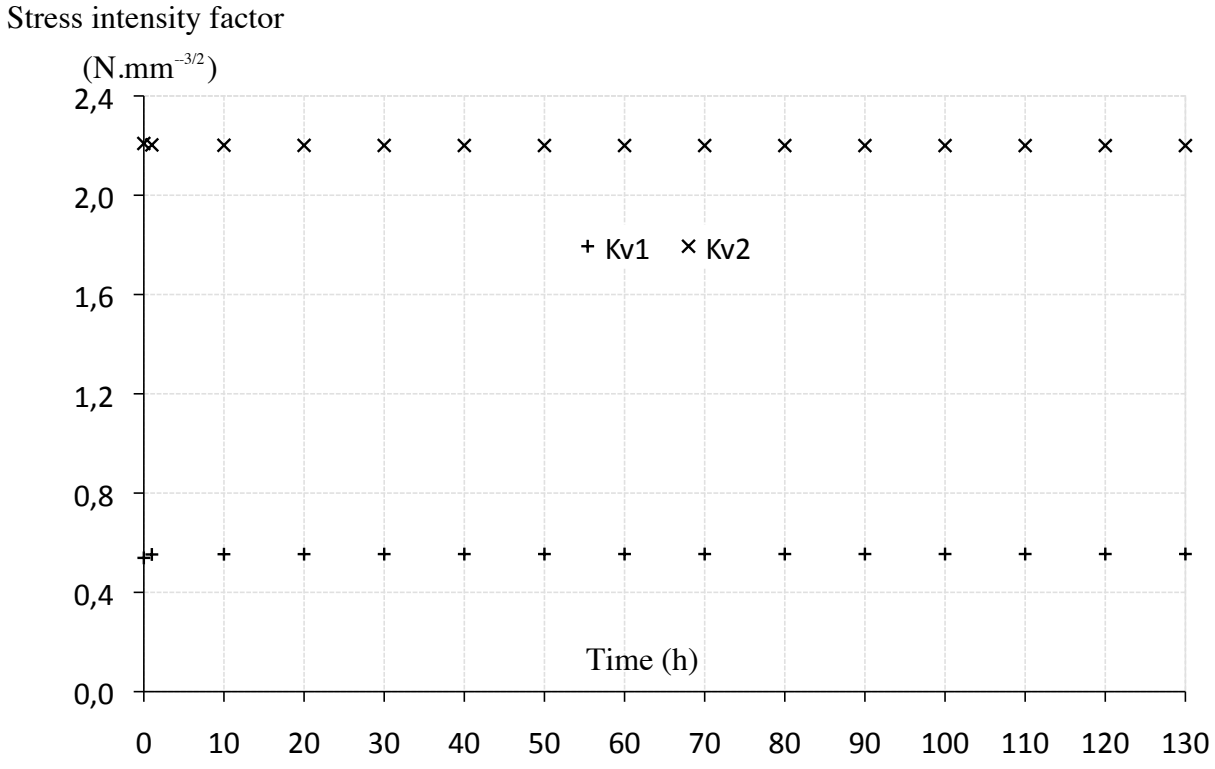

Figure 6 – Stress intensity factor versus time for mixed-mode $\beta = 45°$

Figure 6 presents the evolutions of the viscoelastic stress intensity factors versus time in opening mode *kv1* and in shear mode *kv2* for the mixed-mode loading $\beta = 45$. It observed that the *kv1* is around 0.50 N.mm$^{-3/2}$ and kv2 is around 2.20 N.mm$^{-3/2}$; this values increase slowly after 6 days. The low differences of values prove that the time calculation must be increase in order to obtain the important stress intensity factors. Also, the value of *kv2* is six time more important that *kv1*; this fact is justified by the important energy required by the material to propagate in shear mode comparatively to the opening mode.

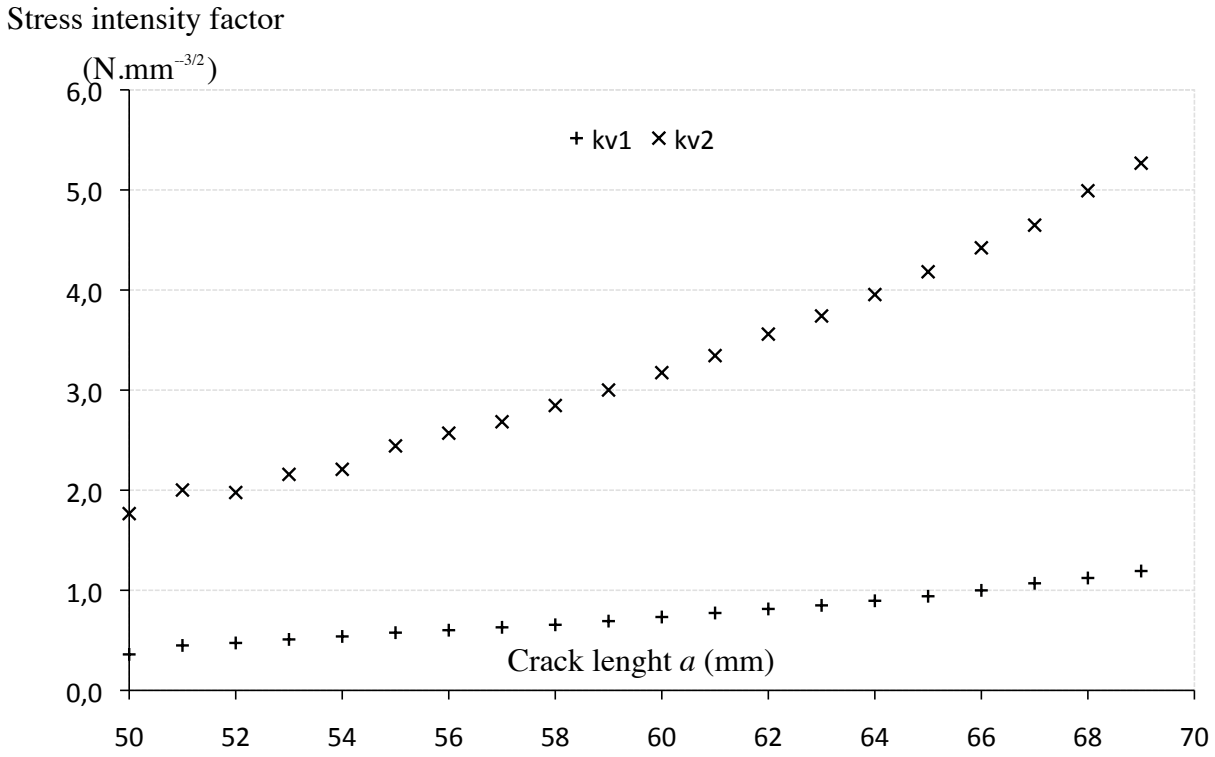

Figure 7 – Stress intensity factor versus crack growth position in mixed-mode $\beta = 45$

Figure 7 presents the evolutions of the stress intensity factors versus crack length *a* in opening mode *kv1* and in shear mode *kv2* for the mixed-mode loading $\beta = 45$. The final crack length is $a = 69\ mm$ and the considered time increment is $\Delta t = 1h$. First, the increasing of stress intensity factors versus crack length is observed. The same evolutions as proposed by Moutou Pitti et al. [16] about viscoelastic energy release rate are obtained. The maximum values of *kv2* vary between 1.77 N.mm$^{-3/2}$ to 5.27 N.mm$^{-3/2}$, and 0.36 N.mm$^{-3/2}$ to 1.19 N.mm$^{-3/2}$ in opening mode, respectively. Note that the initial values at the crack length $a = 50\ mm$ define the critical energy realise rate on the considered material.

7. Conclusion

The evolution of stress intensity factors in viscoelastic orthotropic materials like wood have been investigated in this work. The analytical form of the axisymmetric integral has been developed according to the conservative law and the bilinear free energy density. In order to resolve this integral with finite element software, a modelling form of M_{axi} integral, called $M\theta_{axi}$ has also been proposed and generalized to time dependent materials by $M\theta v_{axi}$. The numerical mixed-mode crack growth has been introduced according the Compact Tension Shear specimen and a specific axisymmetric crack growth plan. The stress intensity factors in mixed-mode $\beta = 45°$ have posted versus time and crack growth for the opening and the shear mode. It observed that the model is efficiency to compute the stress intensity factors in these types of material, but the computational time must be increase. In the coming works, the all mixed-mode ratios must be calculation by taking into account the pressure on the crack lips.

8. References

[1] Moutou Pitti R., Alaa C., Chazal C. Reliability analysis of mixed mode cracking with viscoelastic orthotropic behaviour. Mechanics of Time-Dependent Materials and Processes in Conventional and Multifunctional Materials, Vol. 3. Conference Proceedings of the Society for Experimental Mechanics Series, 2011, Vol. 99999, pp. 249-256, DOI: 10.1007/978-1-4614-0213-8_36

[2] Yasniy P., Maruschak P., Lapusta Y.. Experimental Study of Crack Growth in a Bimetal Under Fatigue and Fatigue-Creep Conditions, International Journal of Fracture. Volume 139, Numbers 3-4, 545-552, DOI: 10.1007/s10704-006-0102-7.

[3] Lapusta Y.N., Henaff-Gardin C., An Analytical Model for Periodic α°-Layer Cracking in Composite Laminates, International Journal of Fracture, Volume 102, Number 3, pp. 73-76, , DOI: 10.1023/A:1007696725543.

[4] Sarler, B.: Axisymmetric augmented thin plate splines. Eng. Analysis Boundary Elements. 21, 81-85 (1998). DOI: 0955-7997/981519.00

[5] Jiang, Q., Gao, C.F.: Axisymmetric stress in an electrostrictive hollow cylinder under electric loading. Acta mech. 211, 309-321 (2010). DOI: 10.1007/s00707-009-0228-6

[6] Yosibash, Z., Hartmann, S., Heisserer, U., Düster A., Rank, E., Szanto, M.: Axisymmetric pressure boundary loading for finite deformation analysis using p-FEM. Comput. Methods Appl. Mech. Engrg. 196, 1261-1277 (2007). DOI:10.1016/j.cma.2006.09.006

[7] Thibauta B., Gril J., Fournier M. Mechanics of wood and trees: some new highlights for an old story, Mécanique du bois et biomécanique des arbres : nouveaux regards sur une vieille question. CR Mecanique, 329, 701-716, 2001.

[8] Atkinson C., Eftaxiopoulos D.A. Crack tip stress intensities in viscoelastic anisotropic bimaterials and the use of the M-integral. Int J Fract, 57: 61-83, 1992.

[9] Chalivendra, V.B.: Mixed-mode crack-tip stress fields for orthotropic functionally graded materials. Acta Mech. 204, 51-60 (2009. DOI : 10.1007/s00707-008-0047-1.

[10] Assous, F., Ciarlet Jr, P., Labrunie, S., Segré, J.: Numerical solution to the time-dependent Maxwell equations in axisymmetric singular domains: the singular complement method. J. Comp. Phys. 191, 147-176 (2003). DOI:10.1016/S0021-9991(03)00309-7

[11] Moutou Pitti, R., Dubois, F., Petit, C., Sauvat, N., Pop, O.: A new M-integral parameter for mixed-mode crack growth in orthotropic viscoelastic material. Eng Fract Mech. 75, 4450-4465 (2008). DOI:10.1016/j.engfracmech.2008.04.021.

[12] Moutou Pitti, R., Dubois, F., Petit, C.: Generalisation of T and A integrals to time dependent materials: analytical formulations. Int. J. Fract. 161, 187-198 (2010). DOI 10.1007/s10704-010-9453-1.

[13] Ormarsson S., Dahlblom O., Petersson H. Numerical study of the shape of Sawn timber subjected to moisture variation, Part 1 : Theory. Wood Sci Technol, 32, 325-334, 1998.

[14] Chen, F.M.K., Shield, R.T.: Conservation laws in elasticity of J-integral type. J. Appl. Mech. Phys. 28, 1-22 (1977).

[15] Noether, E.: Invariant variations problems. Trans Theor Stat Phys. 1, 183-207 (1983).

[16] Moutou Pitti R., Chazal C., Labesse-Jied F., Lapusta Y. A generalization of Mv integral to axisymmetric problems for viscoelastic materials. Acta Mech 220, 365–373 (2011). DOI 10.1007/s00707-011-0460-8

[17] Dubois F., Moutou Pitti R., Picoux B., Petit C. Finite element model for crack growth process in concrete bituminous. Advances in Engineering Software, Vol. 44, No 1, pp. 35-43, 2012. Doi: 10.1016/j.advengsoft.2011.05.039.

[18] Chazal C., Moutou Pitti R. Incremental constitutive formulation for time dependent materials: creep integral approach, Mechanics of Time-Dependent Materials. 15 (3): 239-253, 2011. DOI: 10.1007/s11043-011-9135-z.